Research on Reverse Perspective Principle in the Flight Imaging System

LIU Huiming HE Wanyu SONG Zongquan
Department of Aerial Instrument and Electric Engineering
The First Aeronautical Institute of Air Force
Xinyang, China
liuhm@126.com

***Abstract*—Ordinary flight simulators usually need image in a large number of areas and occupy much more internal storage cells for the flight training. This paper introduces the principle of computerized flight imaging system which was successfully developed by adopting reverse perspective computing method, hardware real-time computation and multistage graphic data base structure. The imaging computer designed by the adoption of the following computing method, hardware computing circuit structure and multi-stage graphic data base satisfactorily solved the problems of computing speed, clipping and filling. Various vivid flight images can be produced under economical conditions.**

***Keywords*—Flight imaging, Reverse perspective computing**

I. MATHEMATICAL MODEL

A. *Mathematical principle of reverse perspective computation*

The coordinate system of reverse perspective computation[1] is shown in "Fig. 1" with the projection screen being fixed and connected to a certain point in front of a plane.

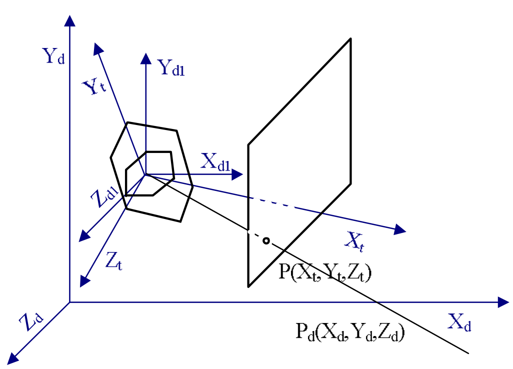

Figure 1. Reverse computing coordinate system.

A scanning spot $P(X_t,Y_t,Z_t)$ can be seen on the screen. The plane moves parallel against the earth coordinates (X_0,Y_0,Z_0) and turns Φ, θ and γ angles. What the computer needs to solve is the color of earth spot $P(X_d,0,Z_d)$ observed by the pilot through $P(X_t,Y_t,Z_t)$. The first task is to conduct rotating transformation of the coordinates. Suppose there exists a mid-coordinate system which parallels the earth coordinate system and whose original point coincides with that of the fuselage coordinates. Consequently, the coordinates of scanning spot $P(X_t,Y_t,Z_t)$ in the coordinate system should be:

$$\begin{bmatrix} X_{d1} \\ Y_{d1} \\ Z_{d1} \end{bmatrix} = \begin{bmatrix} b_{11} & b_{12} & b_{13} \\ b_{21} & b_{22} & b_{23} \\ b_{31} & b_{32} & b_{33} \end{bmatrix} \begin{bmatrix} X_t \\ Y_t \\ Z_t \end{bmatrix} \quad (1)$$

Through projection transformation, the coordinates of spot P_d observed by the via spot $P(X_t,Y_t,Z_t)$ in the mid-coordinate system are computed as:

$$\begin{aligned} X_d &= -Y_0/Y_{d1} \bullet X_{d1} + X_0 \\ Z_d &= -Y_0/Y_{d1} \bullet Z_{d1} + Z_0 \end{aligned} \quad (2)$$

B. *Determination of scanning increment*

In the fuselage coordinate system[2], field scanning is vertically downward and each of the increment in the direction of Y_t is one line as shown in "Fig. 2".

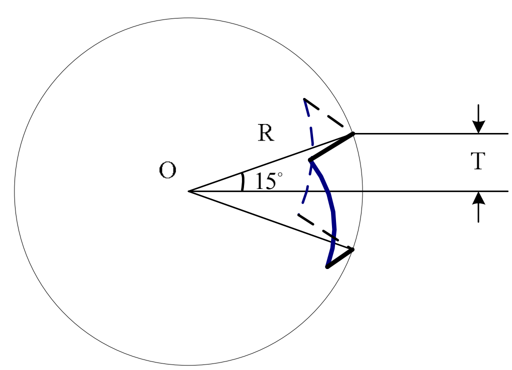

Figure 2. Illustration of scanning increment computation.

$$Y_t = Y_{t0} + \sum \Delta Y_t \quad (3)$$

For each line of scanning, Y_t increases by ΔY_t and Y_{t0} is the height of the starting point of scanning on the left-hand top corner of the screen. If the viewing field angle in vertical direction is 30° and 256 scanning lines are available vertically, the maximum value of hardware in the direction of Y is ±8191, about the same value of spherical radius (R=8191). The extreme value of field scanning Y_t is T when the vertical viewing angle is ±15°, i.e. |T|=8191×Sin15° ≈2119. Field scanning increment ΔY is ΔY =T / 256=± 2119 / 256=±8.27.

The line scanning increment direction parallels with X_t, Z_t plane. The scanning can be disintegrated into two components ΔX_t and ΔZ_t.

$$\begin{aligned} X_t &= X_{t0} + \Sigma \Delta X_t \\ Z_t &= Z_{t0} + \Sigma \Delta Z_t \end{aligned} \quad (4)$$

In the formula, X_{t0} and Z_{t0} are the coordinates of the starting point of scanning, among which line scanning time *t* begins to clear from the starting point of each line.

Suppose the horizontal viewing field angle is 45° (π / 4) and hardware extreme value is ±8191, the number of horizontal scanning spots would be 512. Suppose the in-line increment is M, consequently, M=8191×(π / 4) / 512≈ 12.57

$$\Delta X = M \sin\phi = 12.57 \times \sin\phi$$
$$\Delta Z = M \cos\phi = 12.57 \times \cos\phi$$

ϕ is the included angle between the central normal line of the screen and the X axis of fuselage coordinate system. The above principle will be specified with an example of three-channel image as shown in Fig.3.

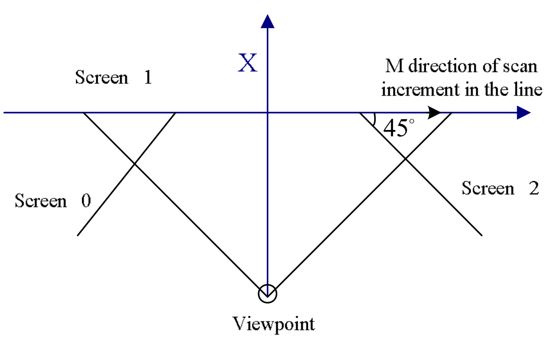

Figure 3. Illustration of three-channel screen position.

As for screen 1, $\phi = 0^\circ$

$$\Delta X = 12.57 \times \sin 0^\circ = 0$$
$$\Delta Z = 12.57 \times \cos 0^\circ = 12.57,$$

As for screen 2 (or screen 0), $\phi = 45^\circ$

$$\Delta X = 12.57 \times \sin 45^\circ = 8.89$$
$$\Delta Z = 12.57 \times \cos 45^\circ = 8.89$$

According to the above deducing, a rational choosing of (X_{t0}, Y_{t0}, Z_{t0}), $(\Delta X, \Delta Y, \Delta Z)$ will help obtain X_t, Y_t, Z_t which is corresponding to scanning and produced by accumulator.

C. Mathematical model

Put (3) and (4) into (1), the following (5) is obtained:

$$\begin{bmatrix} X_{d1} \\ Y_{d1} \\ Z_{d1} \end{bmatrix} = \begin{bmatrix} b_{11} & b_{12} & b_{13} \\ b_{21} & b_{22} & b_{23} \\ b_{31} & b_{32} & b_{33} \end{bmatrix} \begin{bmatrix} X_{t0} + \sum \Delta X_t \\ Y_{t0} + \sum \Delta Y_t \\ Z_{t0} + \sum \Delta Z_t \end{bmatrix}$$
$$= \begin{bmatrix} X_{d10} \\ Y_{d10} \\ Z_{d10} \end{bmatrix} + \begin{bmatrix} \sum (b_{11}\Delta X_t + b_{13}\Delta Z_t) \\ \sum (b_{21}\Delta X_t + b_{23}\Delta Z_t) \\ \sum (b_{31}\Delta X_t + b_{33}\Delta Z_t) \end{bmatrix} + \begin{bmatrix} \sum b_{12}\Delta Y_t \\ \sum b_{22}\Delta Y_t \\ \sum b_{32}\Delta Y_t \end{bmatrix} \quad (5)$$

II. HARDWARE PINCIPLE

A. Hardware computing circuit structure of X_{d1}, Y_{d1}, Z_{d1}

X_{d1}, Y_{d1}, Z_{d1}, same in the expression, can be computed with similar circuit by way of accumulation. "Fig. 4" shows the hardware structure exemplified by X_{d1}computation.

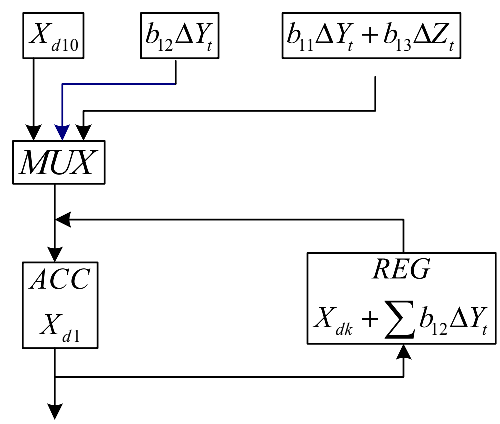

Figure 4. Hardware computing circuit structure of X_{d1}

When field back scanning occurs, X_{d10} is first sent into ACC accumulator, before each line scanning starts, the increment is the direction of $b_{12}\Delta Y_t$ is added into the accumulator and is locked in the REG register. After the starting of scanning, for each clock cycle, ACC conducts accumulation on line scanning increment to produce X_{d1} signal. With the completion of line scanning, the previous line starting point value X_{dk} $(t = k)$ is taken out from REG. X_{d1} is removed and X_{dk}, accumulated by $b_{12}\Delta Y_t$, is again stored in REG and will continue accumulating line scanning increment in the following line.

Computation therefore is simplified by the above mathematical model into three multi-channel accumulators among which the needed X_{d10}, Y_{d10}, Z_{d10}, $b_{12}\Delta Y_t$, $b_{22}\Delta Y_t$, $b_{32}\Delta Y_t$, $b_{11}\Delta X_t + b_{13}\Delta Z_t$, $b_{21}\Delta X_t + b_{23}\Delta Z_t$, $b_{31}\Delta X_t + b_{33}\Delta Z_t$, are computed by a special computer; its result will be used in accumulation.

B. X_d, Z_d hardware computing circuit structure

X_d, Z_d hardware computing circuit structure is shown in "Fig. 5".

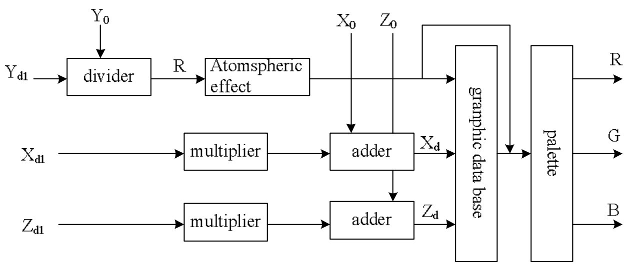

Figure 5. Circuit structure of projection transformation computation.

Proportional projection transformation computation is first done by divider computation $(R = Y_0 / Y_{d1})$ followed by multiplication transformation computation with R to solve $\Delta X_d = R \bullet X_{d1}$, $\Delta Z_d = R \bullet Z_{d1}$ and finally by adder to solve X_d and Z_d. The result thus obtained is the earth coordinates observed by pilot through scanning spot.

III. FLIGHT IMAGE

Ordinary flight simulators[3,4,5] usually need imaged areas of hundreds or over thousands of sq • m for flight training. If each square meter occupies one internal storage cell, one thousand square meters would take up 1M storage cells. As a result, a 100×100 sq • m earth image would require 10000M storage cells. Such a large internal storage proves to be not economical. Since analysis shows that laminations exist in many places on earth and a multi-stage base composed of various laminations will surely save a great deal of repeated data and the storage. For example, when a two-stage base is adopted, its lowest stage using 256 (16×16) color blocks to form a lamination is similar to a Chinese character. A 64K internal storage could store 256 laminations. Advanced bases can, by using 64K storages, combine and edit 256 laminations to produce a page of 4 sq • km earth image, the storage number of which totals 128K, and is only 1 / 128 of the number of the original one-stage base. We adopted the 3 ×3 pixels laminations totaling 256 kinds, capable of six-stage base whose smallest unit is 0.25m×0.25m and can produce 512×512 sq • km earth image.

Experiments show that 256 colors from the base could not meet the actual need, and because atmospheric effect should be added, an adjustment on the colors by supplying a palette circuit is required.

As various liquids and solid particles in the atmosphere might scatter the rays, distant objects could turn grey and fuzzy to devalue the contrast. Distance from eyes to objects should be considered so as to compute atmospheric effect. Analysis based on computation shows that output R of the divider is related to distance. Suppose the fog density is W, a functional relationship of W=F(R) exists in atmospheric effect. A functional table can be made in EPROM and data R is surveyed from EPROM to get W which is sent to color base to control the output of palette. The adopted R is of 6 bit syllable length and can produce 64 levels of visibilities which, if added by 250 color control, can virtually produce 16K effective colors. The W=F(R) relationship is determined by actual testing and experiment.

A sky data base is added to create clouds in the sky. And from the computing analysis, it is known that when $Y_{t1} > 0$, it is the "sky" and Y_{t1} sign bit can be used to switch over earth data base into sky data base. The height of the clouds is obtained by subtracting the height of plane with the bottom height of the clouds which is given by a management computer.

IV. CONCLUSION

The imaging computer designed by adoption of the above-state computing method, hardware computing circuit structure and multi-stage graphic data base satisfactorily solved the problems of computing speed, clipping and filling. Various vivid flight images can be produced under economical conditions.

REFERENCES

[1] A. Sadarjoen, T. van Walsum, A. J. S. Hin, Particle Tracing Algorithms for 3D Curvilinear Grids. Fifth Eurgraphics Workshop on Visualization in Scientific Computing, Rostock, Germany, 5. 1994. 117-120

[2] Hsu P L. Yan W T. Realtime 3D simulation of 3-axis milding using isometric projection. CAD, Vol125 NO.4 1993,71~72

[3] Huang Z, Zhou J. Volume Modeling for Mechanicсal Parts. CADDM, Vol.3, No,1993, 23-40

[4] Zheng F, Ye S H. Volume Graphics Technology. Electronic Science Techonlogy Review, Vol.1, No.1 1994.15-16 .

[5] Nielson G M, et al. Visualization in Scientific Computing. IEEE Computer Society Press. California. 1990. 1131-1136.